Published online 28 September 2017

Nucleic Acids Research, 2017, Vol. 45, No. 22 ***e181***
doi: 10.1093/nar/gkx858

Design and implementation of a synthetic pre-miR switch for controlling miRNA biogenesis in mammals

Janina Atanasov, Florian Groher, Julia E. Weigand* and Beatrix Suess*

Department of Biology, Technical University Darmstadt, Darmstadt 64287, Germany

Received March 21, 2017; Revised August 22, 2017; Editorial Decision September 13, 2017; Accepted September 20, 2017

ABSTRACT

Synthetic RNA-based systems have increasingly been used for the regulation of eukaryotic gene expression. Due to their structural properties, riboregulators provide a convenient basis for the development of ligand-dependent controllable systems. Here, we demonstrate reversible conditional control of miRNA biogenesis with an aptamer domain as a sensing unit connected to a natural miRNA precursor for the first time. For the design of the pre-miR switch, we replaced the natural terminal loop with the TetR aptamer. Thus, the TetR aptamer was positioned close to the Dicer cleavage sites, which allowed sterical control over pre-miR processing by Dicer. Our design proved to be highly versatile, allowing us to regulate the biogenesis of three structurally different miRNAs: miR-126, -34a and -199a. Dicer cleavage was inhibited up to 143-fold via co-expression of the TetR protein, yet could be completely restored upon addition of doxycycline. Moreover, we showed the functionality of the pre-miR switches for gene regulation through the interaction of the respective miRNA with its specific target sequence. Our designed device is capable of robust and reversible control of miRNA abundance. Thus, we offer a novel investigational tool for functional miRNA analysis.

INTRODUCTION

During the last decade, the toolbox of synthetic biology has been filled with a plethora of different genetic parts and devices for the manipulation of cellular function (reviewed in (1,2)). However, the applicability of many of these building blocks is still poorly explored. Even less is known about the genetic modularity and portability of individual tools, thus neglecting the great potential of the combination of different structures to produce switchable elements. The flexible nature of RNA-based systems in particular allows for modular combinations of a riboregulator with virtually every other synthetic or naturally-derived RNA framework, despite the fact that the individual building blocks may have completely different functions. Although several successful attempts demonstrating conditional gene expression with synthetic RNA devices have been published (reviewed in (2,3)), major drawbacks are either the limited repertoire of suitable genetic parts, or the failure to integrate existing parts from different sources into robust frameworks (4). The vast majority of well-characterized regulation systems is tailored for usage in bacteria and lower eukaryotes. However, the full potential of RNA-based regulators for applications in mammalian cells still remains to be accessed (5).

Several recent studies have focused on the significance of small non-coding RNAs for eukaryotic gene regulation and revealed an important role for various biologically relevant processes (reviewed in (6)). To deepen the knowledge about these molecules and their respective functions, the repertoire of existing methods and tools has to be adapted to the specifics of the individual research goal. Such experimental setups would benefit from the use of switchable systems that provide control over the abundance of the respective RNA to investigate its physiological relevance. MicroRNAs (miRNAs) are prime candidates for the development of such switchable systems. This class of non-coding RNAs impacts on post-transcriptional gene silencing in eukaryotes in a process called RNA interference (reviewed in (7)). Acting on translation and mRNA stability, miRNAs influence the functionality of at least 60% of the human protein-coding genes (8). Thus, sequence mutations as well as changes in miRNA abundance often lead to genetic malfunction and may result in a phenotypic appearance (9). Moreover, miRNAs have been identified as the cause of various diseases and show marked tissue specificity. In consequence, they are ideal candidates for biomarker-related early diagnosis and treatment (10). So far, 2500 human miRNAs have been catalogued (miRbase, release 21, http://mirbase.org/), with most of their targets and related functions as yet unknown. In light of the special interest in miRNA function and its involvement in pathogenesis, the development of a specific and universal tool for the regulation of miRNA biogenesis in a ligand-dependent way will provide a useful device to investigate the impact of miRNAs on cellular (mal)function.

*To whom correspondence should be addressed. Tel: +49 6151 1622000; Fax: +49 6151 1622003; Email: bsuess@bio.tu-darmstadt.de
Correspondence may also be addressed to Julia E. Weigand. Tel: +49 6151 1622005; Fax: +49 6151 1622003; Email: weigand@bio.tu-darmstadt.de

Due to their importance for post-transcriptional gene regulation, miRNA biogenesis has to be tightly regulated to guarantee a suitable amount of the functional miRNA. The biogenesis of miRNAs involves two consecutive processing steps to excise the mature miRNA out of a longer primary transcript (pri-miRNA) (reviewed in (7)). Drosha and Dicer, the two key constituents of the processing machinery, together with their auxiliary factors operate with conserved substrate recognition criteria that have to be met for successful processing of the miRNA. For the second maturation step, carried out by the RNase III Dicer, both the sequence of the precursor miRNA (pre-miRNA) and the properties of its terminal loop are relevant (11,12). Dicer acts as a 'molecular ruler', thus the length of the double stranded region in the pre-miRNA and the formation of the typical hairpin structure also contribute to recognition and accurate processing (9,12–14). A structural modification in the pre-miRNA is often accompanied by an imprecise or deficient cleavage, resulting either in an altered seed region or in a total loss of the mature miRNA (12,15). Consequently, the successful design and implementation of a partly synthetic miRNA tool has to meet two requirements: the incorporated switchable element must resemble the original structure of the natural system, and it has to enable a robust ligand-dependent regulation at the same time. Hence, the structural flexibility and the rather small size of an RNA aptamer render it ideally suited to serve as a robust sensor and actuator domain. Aptamers are highly structured oligonucleotides exhibiting high affinity binding to a specific target molecule (reviewed in (16)). The *de novo* selection of an aptamer via SELEX (Systematic Evolution of Ligands by Exponential enrichment) can be performed against virtually any type of ligand ranging from small molecules over proteins up to more complex cellular structures (reviewed in (17)).

To set up a platform for aptamer-controlled pre-miRNA processing, it is desirable to have a system that allows for reversible switching at biologically relevant time scales. Among the many existing aptamer-ligand pairs, the SELEX-derived Tet Repressor (TetR)-binding aptamer and the TetR protein constitute an ideal basis for design and implementation of a reversible miRNA switch. The aptamer has been identified in a combined *in vitro* and *in vivo* selection approach and binds TetR with an extremely high binding affinity (18). The affinity of TetR for the aptamer and the *tetO* operator DNA are equal (19). Binding of tetracycline (tc) or doxycycline (dox), a structural tc analog, to TetR causes a conformational change in the TetR protein core that in turn compromises binding to the aptamer (19), allowing for reversible ligand binding. Both the nature of that RNA/protein/small molecule combination system and the suitable pharmacokinetic properties of both ligands tc and dox are ideally suited for use in mammalian cells and miRNA biogenesis regulation (20).

The applicability of the TetR aptamer system in different organisms has already been confirmed by various approaches. The original publication demonstrated the successful use of the TetR aptamer for controlling gene expression in *Escherichia coli* (18). Next, portability and broader applicability of the system were illustrated with its successful use in the protozoon *Plasmodium falciparum* and in yeast (21,22). Further, an additional layer of regulation was added to the TetR aptamer system with the design of a small-molecule responsive switch that proved functional in mammals (23). These approaches highlight the universal nature and adaptability of the TetR aptamer system.

Most approaches to control RNA interference to date have focused on modified shRNAs for tool development and implementation. The engineering of a complex miRNA-related structure presents a considerable challenge due to the strong dependence on conserved substrate recognition criteria for processing. In contrast to natural pre-miRNAs, shRNAs feature a perfectly hybridized stem topped with a short loop (24). This uncomplicated secondary structure is readily accessible to (i) a specific redesign matching virtually any target sequence, and (ii) to an *in silico* prediction of the Dicer cleavage sites. The modification of an shRNA structure does not require following the strict processing rules that apply to natural pre-miRNAs. Thus, issues associated with the engineering of the considerably more complex structures found in natural pre-miRNAs can be bypassed. The fusion of the *in vitro* selected theophylline aptamer with an shRNA enabled the regulation of Dicer processing and facilitated control over GFP or human albumin levels in a ligand-dependent fashion (25). In a comparable approach, various aptamers together with competing strands were integrated into shRNA loop structures affecting the processing of the respective shRNAs by ligand-dependent switching between two structural conformations (26). Furthermore, protein-binding motifs for the human U1A protein and L7Ae, or the p50-binding aptamer positioned in the shRNA loop region have been shown to regulate shRNA processing by Dicer (27,28). In another design, small molecule or protein-binding aptamers were integrated into the basal segment of a synthetic pri-miRNA bearing an siRNA. Mimicking a pri-miRNA, Drosha processing was controlled, resulting in ligand-dependent control over *GFP* expression (29,30).

The tools above provide valuable proof-of-concept studies. However, they were built based on non-natural engineered structures and still suffer from low dynamic ranges and a lack of regulatory flexibility. Furthermore, the applicability of shRNA-based tools for gene regulation is limited, i.e. they target one specific sequence, whereas miRNAs are capable of binding to several binding sites. RNA interference is increasingly popular as the method of choice for gene-silencing and functional analysis. In consequence, there is an increasing need for robust and reliable interference tools (31). So far, modification of a natural miRNA that resulted in an efficient regulation of mature miRNA levels has not been demonstrated.

Here, we propose an approach for the regulation of natural miRNA systems. With our RNA-based device, we sought to create a universal and reversible switching unit consisting of a synthetic aptamer component as a ligand-sensing domain coupled to a natural pre-miRNA to enable ligand-controlled miRNA abundance (Figure 1). In our system, the TetR aptamer replaces the natural terminal loop of the pre-miR in a way that could be universally employed for different miRNAs. The aptamer is connected to the pre-miRNA stem through a communication module, thus retaining pre-miRNA processing while simultane-

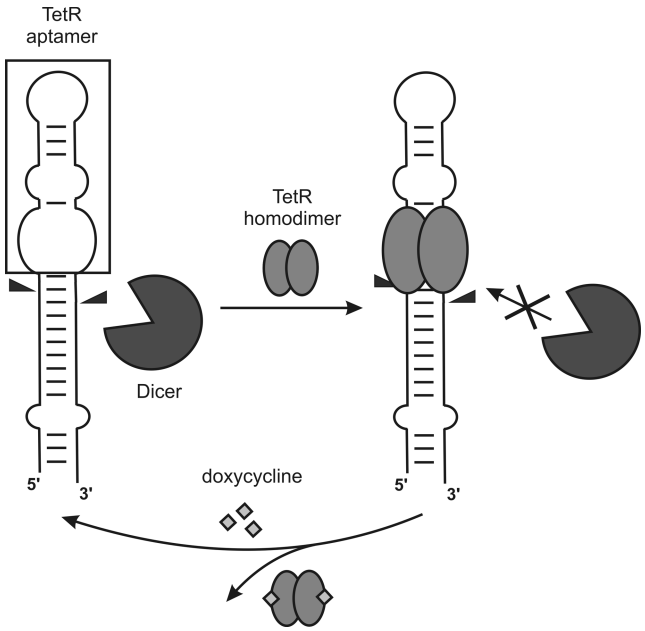

Figure 1. TetR aptamer-dependent regulation of Dicer processing. The TetR aptamer replaces the terminal loop region, acting as the sensor domain of the pre-miR switch. In the absence of the TetR homodimer, Dicer cleaves the pre-miRNA at the indicated processing sites (arrows) leading to the emergence of mature miRNA. Upon expression of the protein, the TetR homodimer binds to the aptamer and blocks the cleavage sites. This, in turn, results in an impairment of Dicer cleavage. The addition of dox to the medium causes the dissociation of TetR from the aptamer, freeing the processing sites. Thus, the pre-miRNA can, once again, be processed to mature miRNA.

ously rendering the system ligand-dependent and reversible. With our pre-miR switch we provide a universally applicable tool that efficiently suppresses miRNA processing with a dynamic range of 40- to 140-fold upon TetR binding. Repression is fully relieved by the addition of dox. Thus, we provide the first evidence for the controlled biogenesis of three different miRNAs using a novel, versatile and flexible synthetic RNA-based regulation system in mammals.

MATERIALS AND METHODS

Cell culture

HeLa cells (DSMZ, No. ACC-57) and HeLa 'Flp-In Host Cell Line' HF1–3 cells (32) were maintained at 37°C in a 5% CO_2 humidified incubator and cultured in Dulbecco's Modified Eagle Medium (DMEM, Sigma Aldrich) supplemented with 10% fetal bovine serum (FBS Superior, Biochrom), 100 U/ml penicillin (PAA, the Cell Culture Company), 100 μg/ml streptomycin (PAA, the Cell Culture Company) and 1 mM sodium pyruvate (PAA The Cell Culture Company). In case of the HeLa HF1–3 cells, 100 μg/ml zeocin (Invivogen) was additionally supplemented to the medium, whereas the medium of the HeLa HF1–3 cells harboring the integrated unmodified miRNA or the pre-miR switch contained 150 μg/ml hygromycin B (Invivogen, Hygromycin B Gold solution).

Genomic integration

For the establishment of a constitutive expression cell line for pre-miR switch 199a_2 and the unmodified control miR-199a, the Flp-In™ System (Thermo Fisher) was used. The constructs together with the TetR expression sequence were cloned into the multiple cloning site of the pcDNA5/FRT plasmid (Invitrogen). The constructs were constitutively expressed from a human cytomegalovirus (CMV) immediate-early enhancer and promoter, whereas TetR was expressed from the SV40 promoter. The plasmids were tested for miRNA-199a and TetR expression and transfected into HF1–3 cells. For transfection, 90 000 HF1–3 cells were seeded in 2 ml of complete medium without selection antibiotics per well in a 12-well plate. In total, 1800 ng of the Flp-recombinase expression vector pOG44 and 200 ng of the construct vector or the control vectors pCMV-MS (33) and pFRT-GFP (34) (ratio 9:1) were transfected using Lipofectamine 2000 (Invitrogen) according to the manufacturer's protocol. After 4 h of incubation, the lipofection mix was removed and 2 ml of complete medium without selection antibiotics were added to each well. Two days after transfection, cells were cultivated in selection medium supplemented with 150 μg/ml hygromycin B. During selection for integrated clones, the selection medium was exchanged every 2–3 days. Selected cells were raised and cultured in T75 cell culture flasks. Genomic integration was confirmed by sequencing.

Transient transfection

HeLa cells were transfected with Lipofectamine 2000 (Invitrogen) according to the manufacturer's protocol. The cells were seeded and incubated for 24 h at 37°C and 5% CO_2, transfected, and again incubated for 24 h at 37°C and 5% CO_2 before RNA isolation.

For RNA isolation, 140 000 cells/well were seeded into 12-well plates. A total amount of 800 ng DNA per well (ratio of miRNA expression plasmid:TetR expression plasmid 1:1) was used for transfection. For luciferase assay, 60,000 cells/well were seeded in 24-well plates. A total DNA amount of 500 ng DNA per well (ratio of reporter gene plasmid: miRNA expression plasmid:TetR expression plasmid:normalization plasmid 4:7:7:2) was used for transfection. After 3 h of incubation at 37°C and 5% CO_2, the medium was replaced with complete growth medium supplemented with 1 μg/μl dox (Sigma Aldrich) or complete medium without further supplements and cells were incubated at 37°C to the next day.

Plasmid construction

For construction of the miRNA expression plasmids, the respective stem-loop structures flanked by 100 nucleotides (nts) up- and downstream of the pri-miRNA-126/ -199a/-34a were amplified from genomic HeLa DNA and introduced into the multiple cloning site of pCMV-MS (33) using XbaI and XhoI restriction sites. Then, the TetR aptamer was introduced using a two-step overlap-extension PCR. The originated amplicon was then introduced into the plasmid employing the restriction sites for XbaI and XhoI,

again. TetR protein expression occurred under control of a CMV promoter with the plasmid pCMV-TetR.

For luciferase assay, either the respective perfect match target sites or a series of three repetitions of the respective natural miRNA target sequence were cloned downstream of firefly luciferase into the pMIR-REPORT vector system using the restriction sites for HindIII/SacI (for perfect match target sites), for HindIII/SacI, SacI/SpeI and SpeI/XhoI (for the naturally derived target sites) and HindIII/SpeI (3′ UTR parts of natural target genes), respectively. As natural target sequence for miRNA-126–3p targeting, the sequence 5′-TTTAACTAAATGTAAGGTACGA-3′ of the 3′ UTR of *SPRED1* was used (35). The target sequence 5′-TTAATTTGTAAACACTGCCA-3′ for miRNA-34a-5p was deduced from the natural target gene *E2F3* (36). For testing the effect of miR-34a on *MET,* the complete 3′ UTR was inserted downstream of the firefly luciferase (37). The natural target sequence 5′-AGAAATATAGGATAGACACTGGA-3′ for miR-199a-5p is *DDR1* derived (http://www.microRNA.org/). For testing a larger part of the 3′ UTR of *DDR1* containing four binding sites for miR-199a-5p, the 3′ UTR was introduced into the vector from position 264–582 (38). For random control construction, the non-binder sequence 5′-GGTCACGGTCACGGTCACGGTC-3′ was introduced instead of the miRNA target sites.

Total RNA extraction

Total RNA was extracted with TRIzol Reagent (Ambion) and washed with trichloromethane (trichlormethan/chloroform ROTIPURAN®, ≥99% pa, Roth) twice. DNA digestion with Turbo DNase (Ambion) was performed according to the manufacturer's protocol. Integrity of the RNA was analyzed on a 1% agarose gel.

Reverse transcription

For the reverse transcription of miRNAs into complementary DNA (cDNA), sequence-specific stem–loop (SL) primers were used to enable target-specific reverse transcription. In total, 100 ng of DNase-treated RNA were transcribed into cDNA. For normalization in qPCR, the small nucleolar RNA (snoRNA) U48 was co-transcribed to cDNA. The reaction mixture/sample contained 1× First-strand buffer (Invitrogen), 50 nM of each SL primer (Sigma Aldrich), 10 μM DTT, 1 μM dNTPs (0.25 μM each dNTP), 5 U/μl Superscript II RT (Invitrogen) in a 10 μl total reaction volume.

The program for reverse transcription contained the following steps: 16°C for 30 min; three successive steps (60 cycles): 30°C for 30 s, 42°C for 30 s, 50°C for 1min; 70°C for 15 min.

The sequences of the SL-primers utilized are given in Supplementary Table S1.

Quantitative real-time PCR

Quantitative real-time PCR (qPCR) was performed according to Chen *et al.* (39) using the Applied BiosystemsStepOnePlus™ Real-Time PCR System (AppliedBiosystems). The program for qPCR consisted of the following steps: 50°C for 2 min; 95°C for 10 min; 40 cycles of 95°C for 15 s and 60°C for 1 min. The reaction mixture/sample contained: 1× TaqMan® Universal PCR Master Mix (Applied Biosystems), 0.5 μM Universal primer and qPCR primer, 1 μl Universal Probe #21 (Roche), 5 μl cDNA (1:5 dilution of the reverse transcription mixture) in a 20 μl reaction volume. The mean of the two technical replicates was used for ΔCt value calculation. The ratio of two cDNAs was calculated through the exponential increase with the formula $2^{-\Delta Ct}$. The ΔCt value represents the difference between $Ct_{reference\ gene}$ and $Ct_{target\ gene}$. Both the means and standard deviations were calculated from three independent biological replicates. The experiments were performed in two technical replicates, $n = 3$.

The sequences of the primers utilized are given in Supplementary Table S2.

Next generation sequencing

HeLa cells were transfected with the respective natural precursor harboring plasmids (pCMV-miR-34a/ pCMV-miR-199a) or the respective pre-miR switch harboring plasmids (pCMV-miR-34a_2/ pCMV-miR-199a_2) and total RNA was isolated (see above for transfection and RNA extraction protocols). For library preparation with the NEBNext® Multiplex Small RNA Library Prep Kit for Illumina (New England Biolabs), the RNAs from the two controls and the RNAs from the two pre-miR switches were pooled. After PCR amplification, mature miRNAs were size-selected using a 6% polyacrylamide gel.

Sequencing was performed on a NextSeq 500 (Illumina) obtaining 150 nt single-end reads (Core Unit Systems Medicine, University of Würzburg). About 45 Mio. reads were obtained for each library. miRNA cleavage patterns were verified using the following bioinformatic pipeline: After assessing the quality of the sequence run with FastQC (http://www.bioinformatics.babraham.ac.uk/projects/fastqc/). We removed the 3′ adapter sequence with cutadapt (40), then re-evaluated library quality with FastQC. miRNAs 199a-5p, 199a-3p and 34a-5p were researched in both libraries, allowing for two mismatches, with programs based on an available software from the Seidman group (41). After extracting the different miRNAs, Clustal omega was used to align the sequences (42). Finally, the frequencies were summed up and normalized to the highest read count for each miRNA for each miRNA and nucleotide position. Within the control library, we detected 134,461 reads for miR-199a-5p, 475,977 reads for miR-199a-3p and 34,051 reads for miR-34a-5p. In the pre-miR switch containing library, we detected 52,322 reads for miR-199a-5p, 148,917 reads for miR-199a-3p and 8,372 reads for miR-34a-5p. Sequencing data are available upon request.

Luciferase assay

The Dual-Glo® Luciferase Assay System (Promega) was used for the luciferase assay according to the manufacturer's protocol. The pMIR-REPORT plasmid (Ambion) that

constitutively expresses the firefly luciferase gene through the CMV promoter was used. The pRL-SV40 (Promega) that provides constitutive expression of the wildtype *Renilla* luciferase gene through the SV40 promoter was co-transfected with the pMIR-Report vector and used as an internal control for the normalization of the firefly luciferase reporter gene values. The respective miRNA target and control sequences or larger parts of the target gene UTRs were introduced into the 3′ UTR of the firefly luciferase reporter gene. The firefly reporter gene plasmids were co-transfected into HeLa cells with the respective miRNA and TetR expression plasmids and the *Renilla* luciferase plasmid for subsequent cultivation in the absence or presence of dox. Duplicate of triplicate measurements were performed 24 h after transfection with the Infinite® M200 plate reader using one second integration time.

First, all firefly luciferase expression values were normalized to *Renilla* luciferase expression values. Second, means were calculated from the measured duplicates or triplicates for every biological replicate. Means were related to the respective mean derived from transfection with the empty vector pCMV-MS instead of a miR overexpression plasmid. Finally, the calculated values resulting from pre-miR switch expression without TetR and dox were defined to equal 1 as a reference for standardization of all values in the presence of TetR ± dox. Both the means and standard deviations were calculated from three independent biological replicates. The experiments were performed in duplicates (miR-199a) or triplicates (miR-126 and miR-34a), $n = 3$.

Time course experiments

The time course experiments were performed using construct miR-199a_2 for transient transfection. To gain information about the precursor processing of the construct over the course of time, additional control transfections with just the construct without the TetR expression plasmid were carried out. After transfection, cells were incubated in complete medium for one day. The next day, 1 μg/μl dox was added to the wells and cells were harvested after 0, 2, 4, 8, 16 and 24 h of incubation at 37°C. Then RNA was isolated from the respective samples and the miRNA amount was determined using qPCR. Finally, the values were normalized to the respective control values reported above. Both the means and the respective standard deviations were calculated from three independent biological replicates. The experiments were performed in two technical replicates, $n = 3$.

Sodium dodecyl sulfate polyacrylamide gel electrophoresis (SDS-PAGE) and western blotting

The expression of TetR after genomic integration was confirmed with western blotting. For SDS-PAGE, Any kDMini-PROTEAN® TGX Stain-Free™ precast gels were used. The protein amount was adjusted to 40 μg protein per sample, mixed with 4x protein loading buffer and heated to 95°C for 5–10 min. The SDS-PAGE gels were run with 140 V in 1× Laemmli buffer.

For western blotting, the Trans-Blot® Turbo™ Transfer system was utilized according to the manufacturer's protocol. Total protein was blotted to a PVDF membrane using the Trans-Blot® Turbo™ Mini PVDF transfer pack (0.2 μm PVDF, Bio-Rad). After blotting the proteins to the membrane, the membrane was blocked with 2% (w/v) ECL Prime blocking reagent (Amersham) in 1× TBST for 1.5 h. The anti-TetR antibody (C. Berens, FAU Erlangen) was used in a 1:5000 dilution, the anti-β-actin (Sigma-Aldrich) in a 1:7000 dilution. Detection was performed with the Clarity™ Western ECL Blotting substrate (Bio-Rad).

RESULTS AND DISCUSSION

Variations in the communication module affect processing and switching efficiency

The goal of this study was to identify a universal design for a pre-miR switch that allows the reversible and efficient control of miRNA levels dependent on the presence of a ligand. To show genetic modularity of our system, we chose the three human miRNAs miR-126, -34a and -199a due to their structural diversity and their clinical importance in disease development (Figure 2) (43–45).

Since we sought to control the processing of pre-miRNAs by Dicer, we replaced the natural terminal loop with the TetR aptamer and connected it by a communication module to the precursor stem (Figure 2). Due to the proximity of the TetR binding site to the Dicer cleavage sites (indicated by arrows in Figure 2), we expected to gain control over Dicer activity through the creation of a sterical hindrance, i.e. by ligand binding to the aptamer. Hence, the presence and absence of TetR determines Dicer accessibility to its substrate (Figure 1).

Because stem stability of the TetR aptamer is of utmost importance to preserve its functionality, we varied nucleotide (nt) identity and stem length as well as stem flexibility in the shared region between the aptamer and the stem region of the pre-miRNA (18). In addition to aptamer function, we had to take into account the optimal distance of the ligand binding site to the Dicer cleavage sites to maximize inhibition efficiency, but still allow for correct processing in the absence of a ligand.

In our first designs, we tried to find a compromise between these two requirements and developed different potential pre-miR switches based on miRNA-126. For the design of construct miR-126_NL, we decided to retain the lower part of the natural terminal loop structure of miRNA-126 in the transition area between precursor stem and the aptamer to mimic the natural loop structure as closely as possible. To further stabilize the aptamer closing stem, an additional C–G base pair (bp) was attached to the natural structure to connect the aptamer to the precursor. In construct miRNA-126_2, we shortened the transition region to decrease the distance between the Dicer cleavage site and the TetR binding site. Furthermore, we enhanced stability by introducing base pairing, with the exception of a small 1 bp mismatch. In contrast to that, miR-126_5l features a fully complementary transition area between precursor stem and aptamer. MiR-126_5 with a communication module of only 1 bp further increases the proximity of the TetR binding site to the Dicer cleavage sites. The functionality of hybrid constructs as a pre-miR switch strongly depends on the linker domain between the inherently different

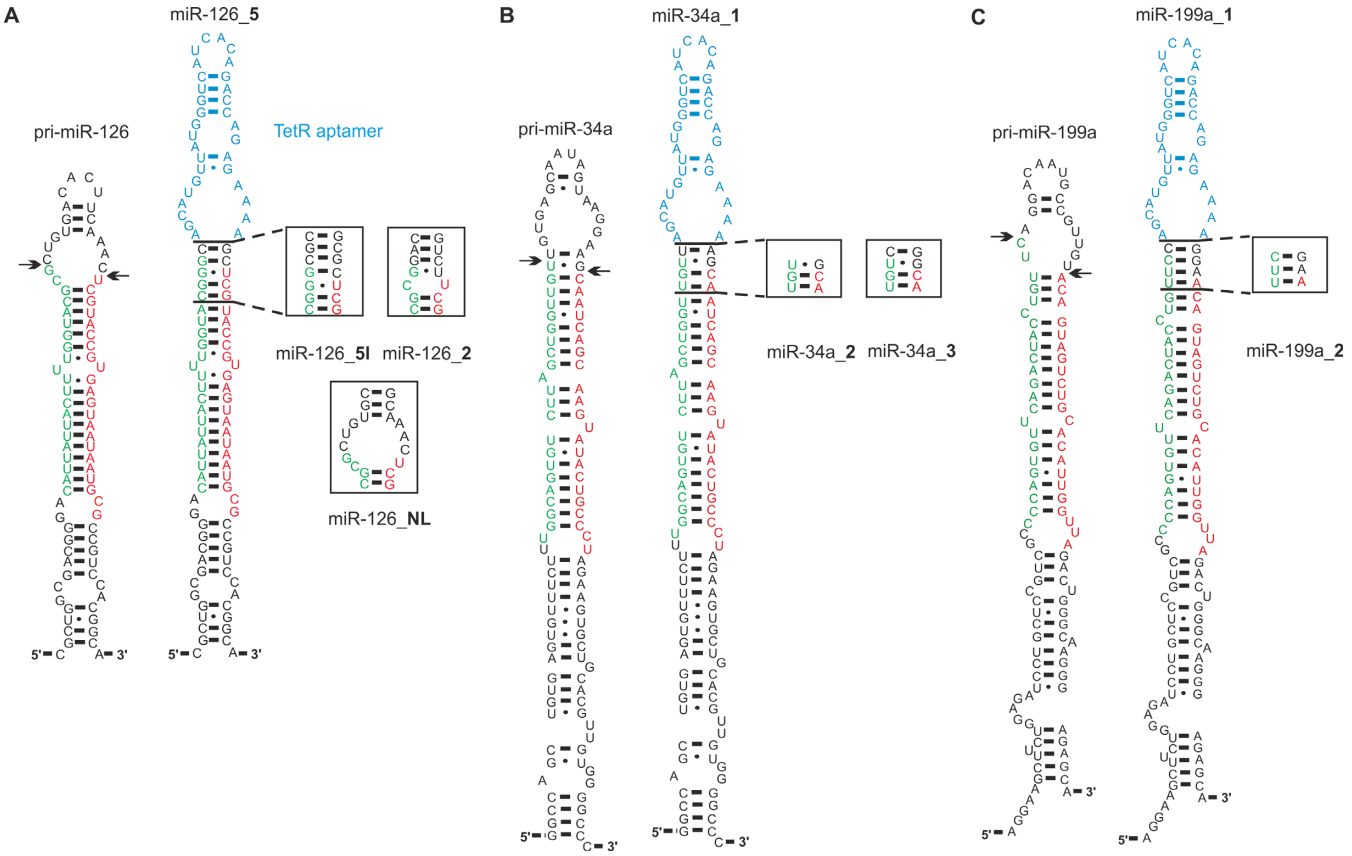

Figure 2. Design of pre-miR switches. Predicted secondary structures of parts of the respective natural pri-miRNAs and the pre-miR switches for (**A**) miR-126, (**B**) miR-34a and (**C**) miR-199a with variations in the communication module between precursor stem and TetR aptamer (blue). The transition area between miRNA precursor and the aptamer is highlighted in boxes. MiRNA-5p is shown in green, whereas red designates miRNA-3p. Arrows indicate the Dicer cleavage sites.

molecules. As already demonstrated, the distance between the protein-binding motif and the Dicer cleavage sites plays an important role for the functionality and efficiency of the tool (27).

In the assays, miRNA-3p and -5p, i.e. the major processing products, were measured for miR-126 and miR-34a, respectively. Because of their clinical importance, the levels of both miR-199a-5p and -3p were assessed. HeLa cells were used because of their low endogenous expression of all tested miRNAs. All constructs are framed by their natural context of 100 nt up- and downstream to preserve folding of the native miRNA structure. All constructs were expressed under the control of a CMV promoter. To analyze the influence of the aptamer fusion on the expression level, expression of mature miR-126 from the pre-miR switches was compared to the respective natural transcript without aptamer in its terminal loop. HeLa cells were transfected with the respective plasmids and total RNA was isolated after 24 h. The amount of mature miR-126–3p was assessed by qPCR. While the constructs miR-126-NL, -2 and -5l showed very low expression levels with a maximum of 3% (Supplementary Figure S1), the expression of construct miR-126_5 was much stronger with ∼23% compared to the unmodified control (Figure 3A).

The design of the pre-miR switches for miR-34a and miR-199a occurred in analogy to miR-126_5, which turned out to provide the best basis for the design of an efficient pre-miR switch. Furthermore, the communication module was varied by either removing the connecting bp (Figure 2 miR-34a_2, miR-199a_2) or exchanging the C–G with an A–U bp (Figure 2 miR-34a_1), to test the flexibility of the communication module.

The amount of mature miRNA of the tested pre-miR switches ranges from 12–35% compared to the unmodified control that is naturally processed by Dicer. For the three miR-34a constructs, we observed a very similar expression level (∼13%, Figure 3B and Supplementary Figure S2), whereas the two modifications in miR-199a_1 and _2 based on a one bp difference yielded about 10% difference in basal expression (Figure 3C).

The replacement of the terminal loop with the aptamer and the composition of the communication module affected miRNA processing to different extents. It is a common phenomenon that the insertion of an aptamer structure, i.e. a stable secondary structure, causes an impairment of expression (reviewed in (46)). However, the adaptation of promoter strength is an adequate counter-measure to increase the respective expression level according to the experimental demand. In all constructs, a flexible, single-stranded terminal loop was replaced by a pre-formed secondary structure. A large, flexible loop structure is generally favored by Dicer, and a certain flexibility seems to be a relevant cri-

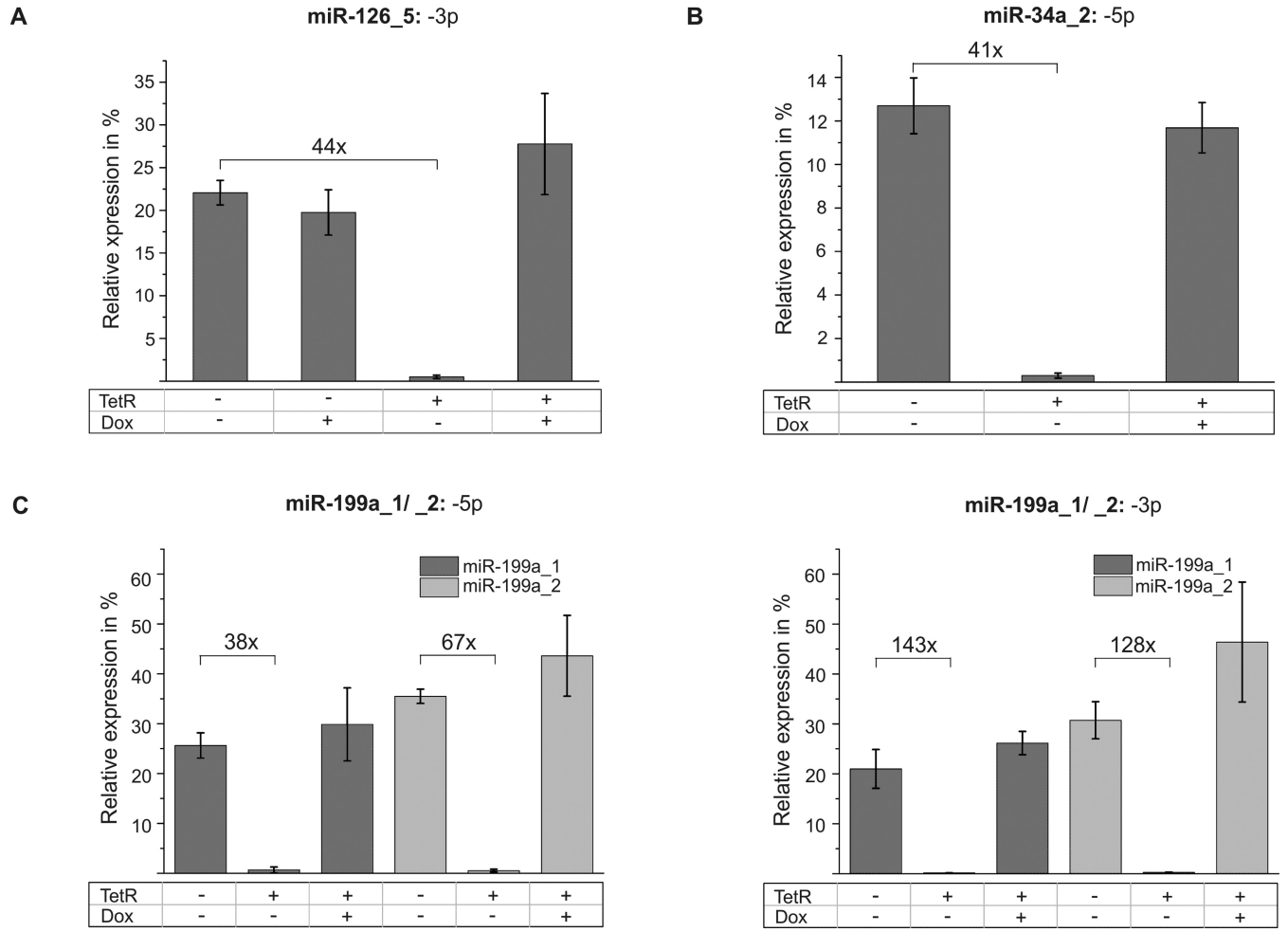

Figure 3. Effect of TetR and dox on mature miRNA abundance. Results of qPCR measurements of the pre-miR switches miR-126_5 (**A**), miR-34a_2 (**B**) and miR-199a_1 and _2 (**C**). HeLa cells were transfected with a plasmid either harboring the unmodified miRNA construct or a pre-miR switch and the TetR expression plasmid. Dox was added to the medium 3 h after transfection. The qPCR-based measurements were performed in two technical replicates 24 h after transfection. Means were calculated from three independent biological replicates. The error bars show the standard deviation. Shown is the amount of mature miRNA derived from the pre-miR switch constructs relative to the miRNA amount derived from the natural miRNA constructs.

terion to facilitate pre-miRNA processing due to granting access of single-stranded sequences to RNA binding proteins (12,47). It was shown that Dicer processing is sensitive to the presence and the position of secondary structures like small bulges in the precursor stem (15). Thus, the presence of the small one bp mismatch next to the Dicer cleavage site present in pre-miR switch miR-126_2 might be responsible for the decreased level of mature miRNA. Furthermore, all of the constructs displaying low expression were designed with a three bp communication module. In all likelihood, this creates an extended substrate with an inappropriate stem length for Dicer processing.

Given the expression profiles of constructs miR-126_5, -34a_1/_2/_3 and -199a_1/_2, we tested the switching behavior of these constructs in the presence of TetR and in the combination of TetR with dox as inducer molecule. For the analysis of the switching efficiency of the constructs, HeLa cells were transfected with the plasmids containing the constructs or the respective natural miRNA together with a TetR expression plasmid. 1 μg/μl dox, an amount of inducer molecule that is typically used for the regulation of TetR controlled systems, was added to the medium 3 h after transfection to test the reversibility of TetR-induced inhibition of pre-miRNA processing. All pre-miR switches showed a significant switching behavior between 41- and about 400-fold in the presence of TetR (Figure 3 and Supplementary Figure S2). This effect is fully reversible with dox. Dox itself has no effect on miRNA precursor processing (Figure 3A). The expression level for each tested miRNA in the presence of TetR was almost as low as the background level, thus indicating the high potential of the developed pre-miR switches.

We performed next generation sequencing to verify that the pre-miR switches produce full-length mature miRNAs. Comparison of the miRNAs produced from pre-miR switches miR-199a_2 and miR-34a_2 to their respective unmodified controls revealed that the fusion of the TetR-aptamer to the miRNA precursor stem did not significantly alter the mature miRNA sequence (Supplementary Figure S3).

Natural terminal loops of some miRNAs usually harbor specific recognition motifs that are important for efficient

substrate recognition and processing regulation, and therefore modifications of that region may affect processing efficiency (48). However, our data clearly demonstrate that functional pre-miR switches can be created on the basis of our design principles, as all three tested miRNAs tolerate the exchange of their natural terminal loop with the TetR aptamer without loss of function.

Our results suggest design rules for the creation of a ligand-dependent pre-miR switch. A communication module that consists of one canonical bp between miRNA precursor stem and aptamer, or even the direct fusion of the two RNA building blocks resulted in the best processing for all tested pre-miR switches. Furthermore, the short communication module exhibits sufficient stem stability to permit aptamer functionality and an appropriate proximity to the Dicer cleavage site to enable efficient processing inhibition. For the pre-miR-199a switches, a higher basal expression was observed for construct 2 for both miRNAs 199a-5p and -3p featuring a direct connection of aptamer and precursor stem. A strong relation between Dicer activity and the base pairing feature of the terminal loop has been shown, since an extension of the stem region negatively affects Dicer processing (12,49,50). Similarly, the direct fusion of the theophylline aptamer to the shRNA resulted in the best regulation of *GFP* expression (25).

Pre-miR switches are fully functional in target gene regulation

Luciferase assays were conducted to demonstrate the functional relevance of the pre-miR switches. The perfect match target sites present the perfect complement to the respective miRNA. They result in complete base pairing of the miRNA with the target sequence and elicit mRNA degradation by cleavage (Figure 4A). Thus, they constitute positive controls to show the maximum effect under the given experimental conditions.

Due to the fact that miRNA binding to a target gene in mammals usually occurs by an imperfect match of miRNA and target sequence (reviewed in (51)), we decided also to integrate natural target sites downstream of the reporter gene (Figure 4B). For that purpose, we chose miRNA binding sequences of target genes that were already validated (35,36,38,52). In total, we cloned one perfect match target site, the 3-fold repetition of a natural binding site, or a full/larger part of the 3′ UTR of respective target genes downstream of the firefly luciferase gene.

A known target of miRNA-126 is *SPRED1*. Its 3′ UTR contains three predicted binding sites for that miRNA. One of these predicted miRNA binding sequences was introduced three times in a row downstream of the luciferase reporter gene (Figure 4B, left). For miR-34a, a predicted binding sequence from the target *E2F3* was used and inserted the same way as for miR-126 (Figure 4B, middle). Furthermore, the *MET* mRNA is a validated target for miR-34a, and therefore the complete natural 3′ UTR was employed to test the pre-miR switch's functionality in a luciferase assay (Figure 4C, left). For the experiments with miR-199a, a 3-fold repetition of a predicted binding site as well as a larger part of the 3′ UTR of *DDR1* containing all of the four predicted miR-199a binding sites were introduced behind the firefly luciferase gene (Figure 4B, right and C right). The binding of the miRNA to the 3′UTR of the respective target genes usually leads to an inhibition of gene expression. Consequently, the level of luciferase expression provides information about the cellular miRNA level that in turn is dependent on the presence of TetR and dox.

Cells were co-transfected with the plasmid containing the respective reporter gene and the pre-miR switch plasmid. In addition, a plasmid harboring a *Renilla* luciferase as transfection control and the TetR expression plasmid were transfected. The luminescence values were normalized to the respective controls that contain the reporter gene plasmid but not the pre-miR switch. To exclude off-target effects, control constructs were generated with one or a triplicate of a non-binding random sequence. Dox was added 3 h after transfection and luminescence values were measured 24 h after transfection.

The data are presented in Figure 4. The luciferase assays with the perfect match binding site downstream of the reporter gene revealed an increase of relative expression between 2.5- and 3.1- fold for the constructs miR-126_5 and miR-199a_2.The increase of relative expression for construct miR-34a_2 with 1.7-fold was more moderate in the presence of TetR (Figure 4A), probably owing to the lower expression level of miR-34a compared to the other two miRNAs. We observed the complete restoration of the relative expression value in the presence of dox for all tested perfect match target sites. The random controls did not show any effect, thus excluding unspecific binding, TetR- or dox-based effects.

When we examined the influence of the pre-miR switches on the constructs with a triplicate of the natural binding site, a dynamic range of 1.5- to 1.9-fold could be observed for all of the tested constructs (Figure 4B). The insertion of the complete *MET* 3′ UTR harboring three different miRNA binding sites for miR-34a led to an increase of relative expression to 1.4-fold (Figure 4C, left), whereas the incorporation of a part of the *DDR1* 3′′ UTR showed a 1.8-fold gain in relative expression due to miR-199a-5p binding (Figure 4C, right). The reversibility of the effect upon dox addition could also be observed in this experimental setup.

Our results confirm that both the expression levels of the miRNAs and the regulation efficiency of the respective pre-miR switches notably influence reporter gene expression, thus supporting observations from qPCR. Binding of the miRNAs to their perfect match binding sites results in a regulation of up to 3-fold for the most highly expressed construct miR-199a_2. A similar effect on *GFP* expression of about 3-fold for the best construct pE19T has been obtained with the theophylline aptamer-based shRNA switch (25). Although less distinct compared to perfect match targeting, binding of the miRNA to the naturally derived binding sequences also resulted in different expression levels of the reporter protein, thus reflecting the robust switching behavior of the pre-miR constructs. Shen *et al*. have introduced a comparable part of the 3′UTR of *DDR1* also harboring all four binding sites downstream of a luciferase reporter gene, and observed a 2.5-fold change in relative luciferase expression in the presence of miR-199a (38). With a 1.8-fold increase of relative reporter gene expression in the presence of TetR, our experiments show regulation in a similar range.

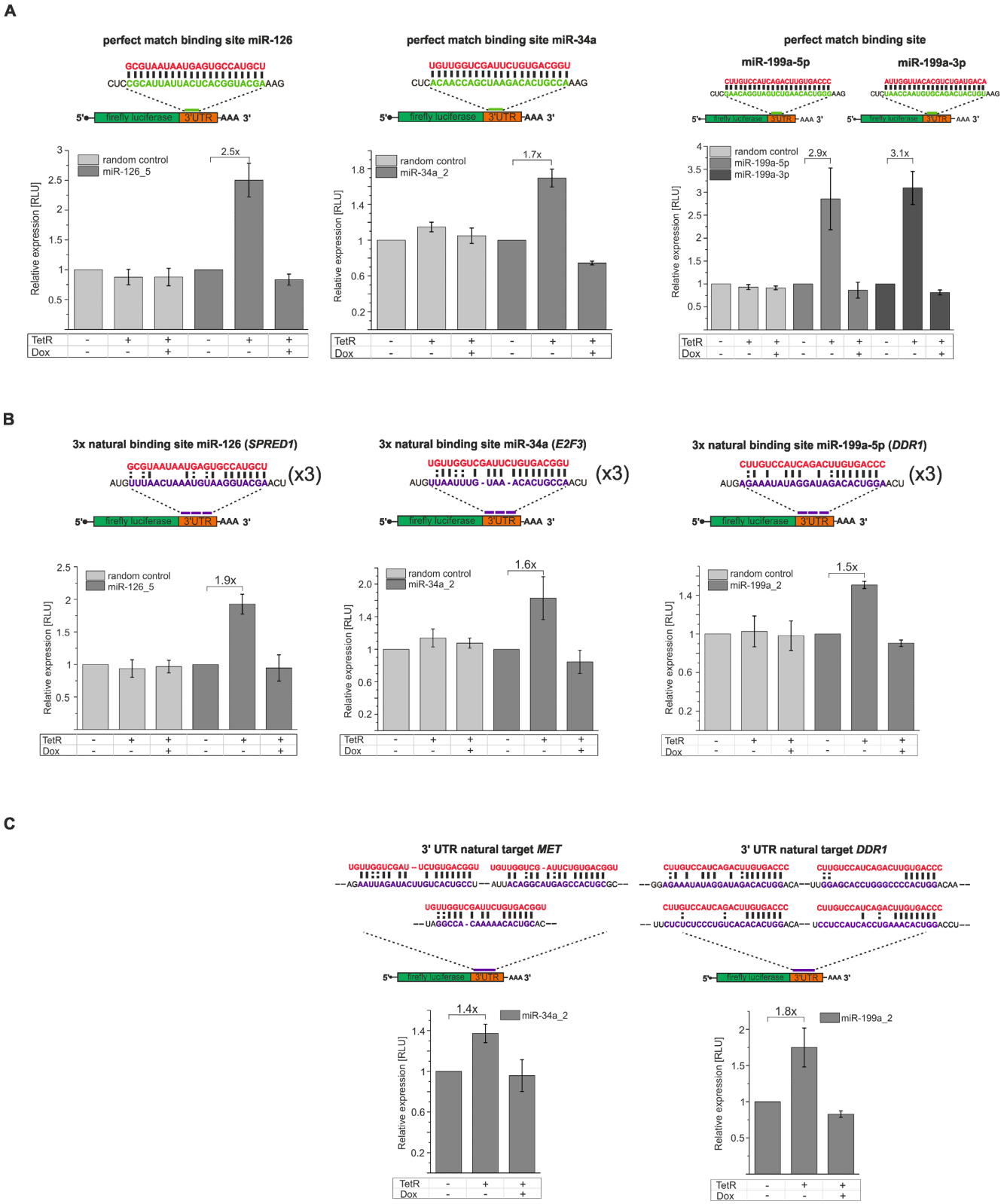

Figure 4. Effect of pre-miR switches on target gene expression. The respective perfect match binding site (**A**), a 3-fold repetition of a binding site derived from a natural target gene (**B**), and a part of the 3′ UTR or the complete 3′ UTR of a target gene (**C**) for miR-126–3p/ -34a-5p and for miR-199a-5p were introduced downstream of a firefly luciferase gene. The miRNA target sequences are either shown in green (A) or in purple (B, C), the miRNA sequences are highlighted in red. HeLa cells were transfected with a reporter gene plasmid either harboring the miRNA target sites or a random control. Furthermore, the plasmids with the natural miRNA or the pre-miR switch, a TetR expression plasmid as well as a *Renilla* luciferase expression plasmid for normalization were co-transfected. Dox was added to the medium 3 h after transfection. Duplicate or triplicate measurements were performed 24 h after transfection ($n = 3$). Means were calculated from three independent biological replicates. The error bars show the standard deviation. Graphs display the relative expression values as x-fold increase normalized to reporter gene expression in the absence of TetR, or dox in the presence of the respective miRNA.

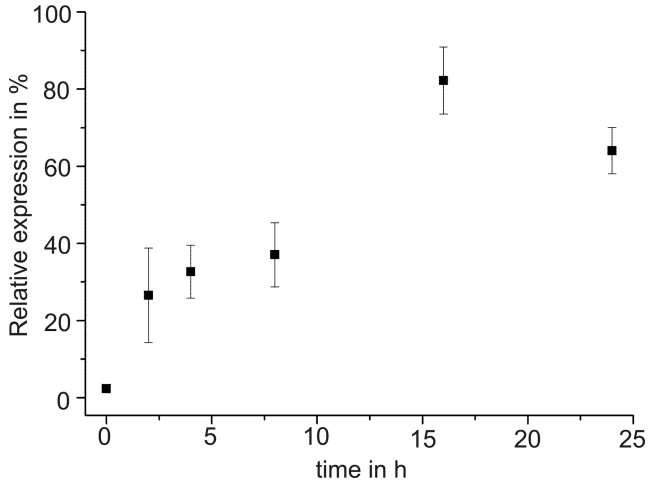

Figure 5. Onset kinetics of pre-miR switch 199a_2. HeLa cells were transfected with a plasmid harboring pre-miR switch miR-199a_2 and the TetR expression plasmid. Twenty four hours after transfection, dox was added to the medium and cells were harvested 0, 2, 4, 8, 16 and 24 h after dox addition. qPCR measurement was performed in two technical replicates for detection of mature miRNA-199a-5p ($n = 3$). Means were calculated from three independent biological replicates. The error bars indicate the standard deviation. Shown is the amount of mature miRNA relative to the miRNA amount derived from controls transfected with the pre-miR switch in the absence of TetR or dox.

Considering the raw data of our reporter gene assays, it is remarkable that the presence of TetR in parallel to the pre-miR switches results in expression levels absolutely identical to the control levels measured in the absence of the respective miRNA. This suggests a full inhibition of the miRNA-target interaction due to TetR and shows that the pre-miR switch is capable of accessing the full potential under the given conditions.

Time course experiments for the determination of the pre-miR switch onset kinetics

Time course experiments were performed to gain information about the onset kinetics of the pre-miR switch miR-199a_2 and, thus, determine the experimental application potential of the switch.

For that purpose, HeLa cells were transiently transfected with the pre-miR switch miR-199a_2. The cells were treated with dox 24 h after transfection. Simultaneously, controls containing just the pre-miR switch construct without TetR and dox were performed to exclude effects caused by transient transfection. The levels of mature miR-199a-5p were measured at 0, 2, 4, 8, 16 and 24 h after dox addition (Figure 5). Results are shown normalized to the respective controls because the control exhibited a reduction of absolute miRNA expression over time that was probably caused by cell division (Supplementary Figure S4).

The results showed a rapid increase of miRNA expression already after 2 h, restoring mature miRNA levels to ∼30%. The steeply increasing expression profile between 0 and 4 h suggests a preceding accumulation of pre-miRNA shielded from degradation probably due to occupation with the TetR protein. Once excessive pre-miRNA is processed by Dicer, miRNA expression kinetics resume a constant expression profile climaxing in the highest measured miRNA amount of 80% at about 16 h after dox addition.

The results suggest that the pre-miR switch miR-199a_2 has fast onset kinetics. An almost complete restoration of miRNA processing was accomplished within 24 h. Hence, the pre-miR switch developed here operates at biologically relevant time scales highlighting its suitability for an application as a robust and efficient miRNA biogenesis regulator.

Pre-miR switch activity after genomic integration

Finally, we aimed to analyze the regulatory performance at single-copy level. For this purpose, we integrated the construct into the genome of the HeLa cell line HF1–3 to explore the functionality of the pre-miR switch after genomic integration. The proof of functionality of the switch after genomic integration is essential for an application of the pre-miR switches in the context of cell lines that stably express TetR. In consequence, long-term studies can easily be performed by regulating miRNA levels simply through the addition of dox.

Stable integration into HF1–3 cells was performed for the pre-miR construct miR-199a_2 and the unmodified miR-199a as a control using the Flp-in® system. TetR was stably integrated along with the respective unmodified miRNA or the pre-miR switch. Cells with the respective integrated constructs were grown for 24 h and dox was added subsequently. The level of the mature miRNA-199a-5p was determined 24 h, 48 h or 5 days after dox addition.

The results indicate that TetR binding to the pre-miR switch resulted in a very low miRNA-199a-5p expression of 1.4% compared to the expression of unmodified miRNA (Figure 6). After adding dox to the medium for 24 h, miRNA expression increased 12-fold. This value remained stable after 48 h. Even after 5 d of incubation, a 9-fold elevation of the amount of mature miRNA up to 15% in comparison to the unmodified control could be shown (Supplementary Figure S5A). These findings correspond with the results obtained from time course experiments and confirm that miRNA processing is completely restored within 24 h of dox incubation. The expression of TetR in HF1–3 cells after genomic integration was confirmed by western Blot (Supplementary Figure S5B).

The fact that the pre-miR switch miR-199a_2 retains considerable switching potential after stable integration is very convenient for further applications. It opens a range of possibilities for long-term miRNA functionality experiments. Furthermore, stable integration offers the advantage of enabling a consistent miRNA expression in every cell, thus equally affecting the whole cell population.

The fast onset kinetics of our pre-miR-based system (Figure 5) suggests an accumulation of pre-miRNA in the presence of TetR. Such an accumulation of double stranded RNA regions may potentially trigger the activation of PKR (protein kinase RNA-activated). PKR is part of the human innate immunity and best known for its role in counteracting viral infection (53). PKR dimerizes on longer stretches of perfect dsRNA, a property typical for viruses and is subsequently activated by autophosphorylation. Once activated, PKR is able to shut down translation by phospho-

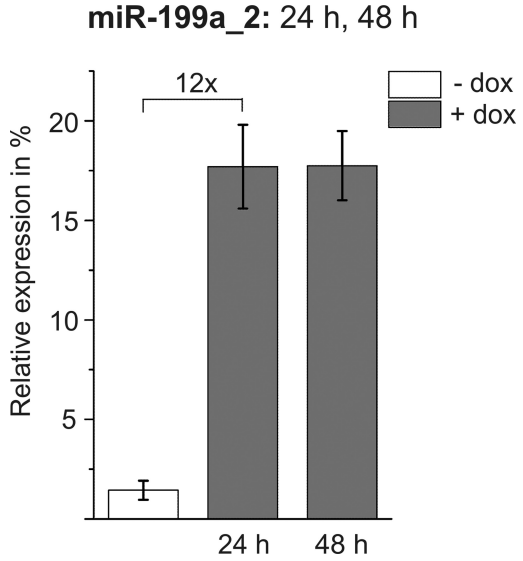

Figure 6. Effect of the chromosomally integrated pre-miR switch on mature miRNA abundance. HeLa HF1–3 cells containing either no construct, the unmodified miRNA or the pre-miR switch together with TetR integrated in the genome were seeded into 12-well plates and incubated for 24h. Then, dox was added to the medium. The qPCR measurements for detection of mature miRNA-199a-5p were performed 24 or 48 h after dox addition in two technical replicates ($n = 3$). Means were calculated from three independent biological replicates. The error bars represent the standard deviation. Shown is the amount of mature miRNA relative to the miRNA amount derived from the unmodified miRNA construct.

rylation of eIF2α. A variety of RNA substrates displaying different structural features have been shown to trigger PKR activation (reviewed in 54). Although miRNA precursors have not been reported to initiate the PKR response so far, we analyzed our data with regard to signs of translation inhibition. However, no effect was observed on cell growth and protein output of cells exhibiting potential pre-miRNA accumulation. Cells stably expressing the pre-miR switch miR-199a_2 and TetR showed no differences in cell growth or protein yield compared to cells stably expressing the unmodified precursor or HF1–3 cells without chromosomal integration. Western blot analysis confirmed the uniform expression of housekeeping genes in the three cell lines (Supplementary Figure S5). Thus, we conclude that a pre-miR switch accumulation in cells does not evoke a general shutdown of translation by induction of PKR.

In sum, our pre-miR switch combined efficiency in with favourable onset kinetics. These characteristics are essential for a fast switch from OFF to ON state. Our design, thus, represents a convenient miRNA switch with broad application potential.

CONCLUSION

Here, we present a robust and reversible RNA-based switching element that allows efficient control of miRNA processing. Previous work documented 'one-way' switching of small non-coding RNA biogenesis to switch off processing through the addition of the respective ligands to aptamer-coupled systems (25,26,28,29,53). However, for short-term interference applications, the operating system must be fully reversible to allow a recovery to the original expression level. The utilization of the TetR aptamer allowed us to design and implement such a reversible system for controlling miRNA biogenesis. Thus, we were able to increase regulatory power and applicability to control cellular mechanisms not only by mimicking miRNA-induced gene knockdown conditions, but also by a subsequent restoration of the mechanism under investigation. Furthermore, we were able to create a concept for the universal design of a pre-miR switch that controlled the processing of three independent and structurally diverse miRNAs. Therefore, it is important to connect the aptamer and a natural miRNA precursor directly or alternatively with a one bp communication module to ensure efficient processing as well as switching activity.

In general, miRNA maturation is distinctly regulated by different protein factors that interact with different parts of the pre-miRs (54–57). These interactions lead to either a blockade or an enhancement of the processing to mature miRNA, and thus exert temporal and spatial control over miRNA levels (58,59). With the work presented here, we promote the idea of an interference with Dicer processing by sterical hindrance through a bulky ligand associated with the pre-miRNA. We demonstrated that this concept is applicable to a natural miRNA system coupled to a TetR-binding aptamer. The design benefits from the reversible character of the TetR-aptamer.

Furthermore, the pre-miR switch extends the versatility of the extensively used TetR system for the conditional expression of miRNAs by introducing a novel layer of regulation at the level of RNA processing. Importantly, our design facilitates miRNA expression in a promoter independent way, which enables to study miRNAs of interest independent of the established TetR-controlled promoters. These are solely based on strong viral or polymerase III-dependent promoters, which interferes and even prevents their use with cell-type or tissue specific expression (60).

As a consequence thereof, the pre-miR switch provides a means to avoid leaky expression often encountered when using inducible promoters. Consequently, its avoidance is a matter of ongoing research (61,62). Leaky expression is thought to arise due to positional effects after genomic integration, for instance because of close proximity to genomic enhancer elements (63). Our pre-miR switch design operates at the RNA level and is therefore unaffected by such interference. It is applicable with genomic TetR integration, which enables its implementation in already existing cell lines.

With the development of a robust and efficient pre-miR switch we present a useful alternative to the classical transcription-based TetR systems, thereby providing a significant expansion of the toolbox for RNAi applications, which may be pivotal to shed further light on the biological role of small non-coding RNAs and their involvement in disease development.

SUPPLEMENTARY DATA

Supplementary Data are available at NAR Online.

FUNDING

Deutsche Forschungsgemeinschaft [SFB902/A2 to B.S., SFB902/B14 to J.E.W.]; LOEWE CGT and CompuGene, EU FP7 PROMYS and ERASynBio "INTENSIFY". Funding for open access charge: BMBF.
Conflict of interest statement. None declared.

REFERENCES

1. McKeague,M., Wong,R.S. and Smolke,C.D. (2016) Opportunities in the design and application of RNA for gene expression control. *Nucleic Acids Res.*, **44**, 2987–2999.
2. Berens,C., Groher,F. and Suess,B. (2015) RNA aptamers as genetic control devices: the potential of riboswitches as synthetic elements for regulating gene expression. *Biotechnol. J.*, **10**, 246–257.
3. Redden,H., Morse,N. and Alper,H.S. (2015) The synthetic biology toolbox for tuning gene expression in yeast. *FEMS Yeast Res.*, **15**, 1–10.
4. Lu,T.K., Khalil,A.S. and Collins,J.J. (2009) Next-generation synthetic gene networks. *Nat. Biotechnol.*, **27**, 1139–1150.
5. Berens,C. and Suess,B. (2015) Riboswitch engineering - making the all-important second and third steps. *Curr. Opin. Biotechnol.*, **31**, 10–15.
6. Esteller,M. (2011) Non-coding RNAs in human disease. *Nat. Rev. Genet.*, **12**, 861–874.
7. Wilson,R.C. and Doudna,J.A. (2013) Molecular mechanisms of RNA interference. *Annu. Rev. Biophys.*, **42**, 217–239.
8. Friedman,R.C., Farh,K.K.H., Burge,C.B. and Bartel,D.P. (2009) Most mammalian mRNAs are conserved targets of microRNAs. *Genome Res.*, **19**, 92–105.
9. Hogg,D.R. and Harries,L.W. (2014) Human genetic variation and its effect on miRNA biogenesis, activity and function. *Biochem. Soc. Trans.*, **42**, 1184–1189.
10. Mishra,P.J. (2014) MicroRNAs as promising biomarkers in cancer diagnostics. *Biomark. Res.*, **2**, 4–7.
11. Starega-Roslan,J., Galka-Marciniak,P. and Krzyzosiak,W.J. (2015) Nucleotide sequence of miRNA precursor contributes to cleavage site selection by Dicer. *Nucleic Acids Res.*, doi:10.1093/nar/gkv968.
12. Zhang,X. and Zeng,Y. (2010) The terminal loop region controls microRNA processing by Drosha and Dicer. *Nucleic Acids Res.*, **38**, 7689–7697.
13. Feng,Y., Zhang,X., Graves,P. and Zeng,Y.A.N. (2012) A comprehensive analysis of precursor microRNA cleavage by human Dicer. *RNA*, **18**, 2083–2092.
14. Vermeulen,A., Behlen,L., Reynolds,A., Wolfson,A., Marshall,W.S., Karpilow,J.O.N. and Khvorova,A. (2005) The contributions of dsRNA structure to Dicer specificity and efficiency. *RNA*, **11**, 674–682.
15. Ma,H., Wu,Y., Niu,Q., Zhang,J., Jia,G., Manjunath,N. and Wu,H. (2016) A sliding-bulge structure at the Dicer processing site of pre-miRNAs regulates alternative Dicer processing to generate 5′-isomiRs. *Heliyon.*, **2**, e00148.
16. Ruscito,A. and DeRosa,M.C. (2016) Small-molecule binding aptamers: selection strategies, characterization, and applications. *Front. Chem.*, **4**, 1–14.
17. Darmostuk,M., Rimpelova,S., Gbelcova,H. and Ruml,T. (2015) Current approaches in SELEX: an update to aptamer selection technology. *Biotechnol. Adv.*, **33**, 1141–1161.
18. Hunsicker,A., Steber,M., Mayer,G., Meitert,J., Klotzsche,M., Blind,M., Hillen,W., Berens,C. and Suess,B. (2009) An RNA aptamer that Induces transcription. *Chem. Biol.*, **16**, 173–180.
19. Steber,M., Arora,A., Hofmann,J., Brutschy,B. and Suess,B. (2011) Mechanistic basis for RNA aptamer-based induction of TetR. *ChemBioChem*, **12**, 2608–2614.
20. Gossen,M., Freundlieb,S., Bender,G., Müller,G., Hillen,W. and Bujard,H. (1995) Transcriptional activation by tetracyclines in mammalian-cells. *Science*, **268**, 1766–1769.
21. Goldfless,S.J., Belmont,B.J., De Paz,A.M., Liu,J.F. and Niles,J.C. (2012) Direct and specific chemical control of eukaryotic translation with a synthetic RNA-protein interaction. *Nucleic Acids Res.*, **40**, 1–12.
22. Goldfless,S.J., Wagner,J.C. and Niles,J.C. (2014) Versatile control of Plasmodium falciparum gene expression with an inducible protein-RNA interaction. *Nat. Commun.*, **5**, 5329.
23. Wieland,M., Ausländer,S., Tigges,M. and Fussenegger,M. (2011) Rational design of a small molecule-responsive intramer controlling transgene expression in mammalian cells. *Nucleic Acids Res.*, **39**, e155.
24. Moore,C.B., Guthrie,E.H., Huang,M.T. and Taxman,D.J. (2010) Short hairpin RNA (shRNA): design, delivery, and assessment of gene knockdown. *Methods Mol. Biol.*, **629**, 141–158.
25. An,C., Trinh,V.B. and Yokobayashi,Y. (2006) Artificial control of gene expression in mammalian cells by modulating RNA interference through aptamer − small molecule interaction artificial control of gene expression in mammalian cells by modulating RNA interference through aptamer – small molecule i. *RNA*, **12**, 710–716.
26. Beisel,C.L., Bayer,T.S., Hoff,K.G. and Smolke,C.D. (2008) Model-guided design of ligand-regulated RNAi for programmable control of gene expression. *Mol. Syst. Biol.*, **4**, 224.
27. Saito,H., Fujita,Y., Kashida,S., Hayashi,K. and Inoue,T. (2011) Synthetic human cell fate regulation by protein-driven RNA switches. *Nat. Commun.*, **2**, 160–168.
28. Kashida,S., Inoue,T. and Saito,H. (2012) Three-dimensionally designed protein-responsive RNA devices for cell signaling regulation. *Nucleic Acids Res.*, **40**, 9369–9378.
29. Beisel,C.L., Chen,Y.Y., Culler,S.J., Hoff,K.G. and Smolke,C.D. (2011) Design of small molecule-responsive microRNAs based on structural requirements for Drosha processing. *Nucleic Acids Res.*, **39**, 2981–2994.
30. Beisel,C.L., Bloom,R.J. and Smolke,C.D. (2014) Construction of ligand-responsive MicroRNAs that operate through inhibition of Drosha processing. *Methods Mol. Biol.*, 259–267.
31. Pekarik,V. (2005) Design of shRNAs for RNAi—a lesson from pre-miRNA processing: possible clinical applications. *Brain Res. Bull.*, **68**, 115–120.
32. Berens,C., Lochner,S., Löber,S., Usai,I., Schmidt,A., Drueppel,L., Hillen,W. and Gmeiner,P. (2006) Subtype selective tetracycline agonists and their application for a two-stage regulatory system. *ChemBioChem*, **7**, 1320–1324.
33. Kemmerer,K. and Weigand,J.E. (2014) Hypoxia reduces MAX expression in endothelial cells by unproductive splicing. *FEBS Lett.*, **588**, 4784–4790.
34. Beilstein,K., Wittmann,A., Grez,M. and Suess,B. (2014) Conditional control of mammalian gene expression by tetracycline- dependent hammerhead ribozymes. *ACS Synth. Biol.*, **4**, 526–534.
35. Fish,J., Santoro,M., Morton,S., Yu,S., Yeh,R., Wythe,J., Ivey,K., Bruneau,B., Stainier,D. and Srivastava,D. (2008) miR-126 regulates angiogenic signaling and vascular integrity. *Dev. Cell*, **15**, 272–284.
36. Welch,C., Chen,Y. and Stallings,R.L. (2007) MicroRNA-34a functions as a potential tumor suppressor by inducing apoptosis in neuroblastoma cells. *Oncogene*, **26**, 5017–5022.
37. Li,N., Fu,H., Tie,Y., Hu,Z., Kong,W., Wu,Y. and Zheng,X. (2009) miR-34a inhibits migration and invasion by down-regulation of c-Met expression in human hepatocellular carcinoma cells. *Cancer Lett.*, **275**, 44–53.
38. Shen,Q., Cicinnati,V.R., Zhang,X., Iacob,S., Weber,F., Sotiropoulos,G.C., Radtke,A., Lu,M., Paul,A., Gerken,G. *et al.* (2010) Role of microRNA-199a-5p and discoidin domain receptor 1 in human hepatocellular carcinoma invasion. *Mol. Cancer*, **9**, 1–12.
39. Chen,C., Ridzon,D.A., Broomer,A.J., Zhou,Z., Lee,D.H., Nguyen,J.T., Barbisin,M., Xu,N.L., Mahuvakar,V.R., Andersen,M.R. *et al.* (2005) Real-time quantification of microRNAs by stem-loop RT-PCR. *Nucleic Acids Res.*, **33**, 1–9.
40. Martin,M. (2011) Cutadapt removes adapter sequences from high-throughput sequencing reads. *EMBnet.journal*, **17**, 10.
41. Eminaga,S., Christodoulou,D.C., Vigneault,F., Church,G.M. and Seidman,J.G. (2013) Quantification of microRNA expression with next-generation sequencing. In: *Current Protocols in Molecular Biology*. John Wiley & Sons, Inc., Hoboken, doi:10.1002/0471142727.mb0417s103.
42. Sievers,F., Wilm,A., Dineen,D., Gibson,T.J., Karplus,K., Li,W., Lopez,R., McWilliam,H., Remmert,M., Söding,J. *et al.* (2011) Fast, scalable generation of high-quality protein multiple sequence alignments using Clustal Omega. *Mol. Syst. Biol.*, **7**, 539.

43. Ebrahimi,F., Gopalan,V., Smith,R.A. and Lam,A.K.Y. (2014) MiR-126 in human cancers: clinical roles and current perspectives. *Exp. Mol. Pathol.*, **96**, 98–107.
44. Ma,W., Xiao,G.G., Mao,J., Lu,Y., Song,B., Wang,L., Fan,S., Fan,P., Hou,Z., Li,J. *et al.* (2015) Dysregulation of the miR-34a-SIRT1 axis inhibits breast cancer stemness. *Oncotarget*, **6**, 10432–10444.
45. Mizuno,S., Bogaard,H.J., Gomez-Arroyo,J., Alhussaini,A., Kraskauskas,D., Cool,C.D. and Voelkel,N.F. (2012) MicroRNA-199a-5p is associated with hypoxia-inducible factor-1 alpha expression in lungs from patients with COPD. *Chest*, **142**, 663–672.
46. Schneider,C. and Suess,B. (2016) Identification of RNA aptamers with riboswitching properties. *Methods*, **97**, 44–50.
47. Castilla-llorente,V., Nicastro,G. and Ramos,A. (2013) Terminal loop-mediated regulation of miRNA biogenesis: selectivity and mechanisms. *Biochem. Soc. Trans.*, **41**, 861–865.
48. Choudhury,N.R. and Michlewski,G. (2012) Terminal loop-mediated control of microRNA biogenesis: selectivity and mechanism. *Biochem. Soc. Trans.*, **41**, 789–793.
49. Chakravarthy,S., Sternberg,S.H., Kellenberger,C.A. and Doudna,J.A. (2010) Substrate-specific kinetics of dicer-catalyzed RNA processing. *J. Mol. Biol.*, **404**, 392–402.
50. Feng,Y., Zhang,X., Graves,P. and Zeng,Y. (2012) A comprehensive analysis of precursor microRNA cleavage by human Dicer. *RNA*, **18**, 2083–2092.
51. Filipowicz,W., Bhattacharyya,S.N. and Sonenberg,N. (2008) Mechanisms of post-transcriptional regulation by microRNAs: are the answers in sight? *Nat. Rev. Genet.*, **9**, 102–114.
52. Li,N., Fu,H., Tie,Y., Hu,Z., Kong,W., Wu,Y. and Zheng,X. (2009) miR-34a inhibits migration and invasion by down-regulation of c-Met expression in human hepatocellular carcinoma cells. *Cancer Lett.*, **275**, 44–53.
53. Dalet,A., Gatti,E. and Pierre,P. (2015) Integration of PKR-dependent translation inhibition with innate immunity is required for a coordinated anti-viral response. *FEBS Lett.*, **589**, 1539–1545.
54. Hull,C.M. and Bevilacqua,P.C. (2016) Discriminating self and non-self by RNA: roles for RNA structure, misfolding, and modification in regulating the innate immune sensor PKR. *Acc. Chem. Res.*, **49**, 1242–1249.
55. Tuleuova,N., An,C.Il, Ramanculov,E., Revzin,A. and Yokobayashi,Y. (2008) Modulating endogenous gene expression of mammalian cells via RNA-small molecule interaction. *Biochem. Biophys. Res. Commun.*, **376**, 169–173.
56. Liu,G., Min,H., Yue,S. and Chen,C.-Z. (2008) Pre-miRNA loop nucleotides control the distinct activities of mir-181a-1 and mir-181c in early T cell development. *PLoS One*, **3**, e3592.
57. Michlewski,G. and Cáceres,J.F. (2010) Antagonistic role of hnRNP A1 and KSRP in the regulation of let-7a biogenesis. *Nat. Struct. Mol. Biol.*, **17**, 1011–1018.
58. Rybak,A., Fuchs,H., Smirnova,L., Brandt,C., Pohl,E.E., Nitsch,R. and Wulczyn,F.G. (2008) A feedback loop comprising lin-28 and let-7 controls pre-let-7 maturation during neural stem-cell commitment. *Nat. Cell Biol.*, **10**, 987–993.
59. Ray,P.S., Jia,J., Yao,P., Majumder,M., Hatzoglou,M. and Fox,P.L. (2009) A stress-responsive RNA switch regulates VEGFA expression. *Nature*, **457**, 915–919.
60. Aagaard,L., Amarzguioui,M., Sun,G., Santos,L.C., Ehsani,A., Prydz,H. and Rossi,J.J. (2007) A facile lentiviral vector system for expression of doxycycline-inducible shRNAs: knockdown of the pre-miRNA processing enzyme Drosha. *Mol. Ther.*, **15**, 938–945.
61. Chen,X., Li,T., Wang,X., Du,Z., Liu,R., Yang,Y., M,N.Z., M,A.C. and P,L.R. (2016) Synthetic dual-input mammalian genetic circuits enable tunable and stringent transcription control by chemical and light. *Nucleic Acids Res.*, **44**, 2677–2690.
62. Adams,F.F., Heckl,D., Hoffmann,T., Talbot,S.R., Kloos,A., Thol,F., Heuser,M., Zuber,J., Schambach,A. and Schwarzer,A. (2017) An optimized lentiviral vector system for conditional RNAi and efficient cloning of microRNA embedded short hairpin RNA libraries. *Biomaterials*, **139**, 102–115.
63. Pinto,R., Hansen,L., Hintze,J., Almeida,R., Larsen,S., Coskun,M., Davidsen,J., Mitchelmore,C., David,L., Troelsen,J.T. *et al.* (2017) Precise integration of inducible transcriptional elements (PrIITE) enables absolute control of gene expression. *Nucleic Acids Res.*, **45**, e123.